J. Membrane Biol. 169, 29–38 (1999)

The Journal of
Membrane
Biology

Nonselective Cation Channels in Endothelial Cells Derived from Human Umbilical Vein

M. Kamouchi, A. Mamin, G. Droogmans, B. Nilius
Laboratorium voor Fysiologie, Campus Gasthuisberg, KU Leuven, B-3000 Leuven, Belgium

Received: 13 October 1998/Revised: 28 January 1999

Abstract. (i) We have used a combined patch-clamp and fura-2 fluorescence technique to characterize a nonselective cation channel (NSC) in Ea.hy926 (EA) cells, an endothelial cell line derived from human umbilical vein. (ii) Stimulation with ATP, histamine and bradykinin activated slowly and with a long delay after application of the agonist, a nonselective cation current (I_{NSC}) which is time- and voltage-independent. The permeability sequence for cations was $P_{Na} > P_{Cs} >> P_{NMDG}$, P_{Ca}. In the absence of external Ca^{2+} and at rather high concentrations, La^{3+} and Gd^{3+} blocked I_{NSC}. (iii) Single channel analysis revealed that ATP activates in the cell-attached configuration a nonselective cation channel with a conductance of approximately 24 pS and a permeation sequence identical to that of the macroscopic current. The channel activity disappeared after membrane excision. (iv) Activation of NSC required physiological intracellular Ca^{2+} levels (100 nM or higher). All agonists failed to activate NSC if cytosolic Ca^{2+} ($[Ca^{2+}]_i$) was lowered by 10 mM BAPTA. Clamping internal Ca^{2+} at 1 μM sometimes (8 out of 17 cells) spontaneously activated I_{NSC} in the absence of any additional stimulus. (v) Application of 2,5-di-*tert*-butylhydroquinone and internal perfusion of inositol 1,4,5-trisphosphate also activated I_{NSC}. The phospholipase C inhibitor, U-73122 inhibited I_{NSC} and the sustained Ca^{2+} plateau during agonist stimulation whereas the inactive analogue, U-73343 had no effect. (vi) These results indicate NSC may act as a Ca^{2+} entry pathway in endothelium. $[Ca^{2+}]_i$ and inositol 1,4,5-trisphosphate play a role in the activation cascade of NSC, and possibly also store depletion.

Introduction

The elevation of cytosolic Ca^{2+} ($[Ca^{2+}]_i$) plays a key role in various cellular functions including the synthesis and release of vasoactive substances in endothelium (Inagami, Naruse & Hoover, 1995; Iouzalen et al., 1996; Lantoine et al., 1998). Agonists have been shown to induce a rapid increase in $[Ca^{2+}]_i$ due to the release of Ca^{2+} from inositol 1,4,5-trisphosphate ($Ins(1,4,5)P_3$) sensitive stores followed by transmembrane Ca^{2+} influx (Berridge, 1995; Clapham, 1995; Nilius et al., 1998).

The elucidation of the various Ca^{2+} entry pathways in endothelial cells (EC) is still in its infancy. Two classes of Ca^{2+} permeable channels responsible for Ca^{2+} influx during stimulation have been described, i.e., store operated Ca^{2+}-selective ion channels and second messenger operated nonselective cation channels. To the first class belong the Ca^{2+} release activated Ca^{2+} (CRAC) channels which were initially characterized in mast cells as highly Ca^{2+}-selective store operated channels (Hoth & Penner, 1992, 1993). It is accepted that CRAC channels play a functional role for Ca^{2+} influx activated by store depletion in nonexcitable cells, including EC (Berridge, 1995; Fasolato & Nilius, 1998; Nilius, Viana & Droogmans, 1997; Oike et al., 1994; Parekh & Penner, 1997). On the other hand, nonselective cation channels (NSC) are of considerable interest since they are also believed to play a key role in Ca^{2+} influx in endothelium (Baron et al., 1996; Kamouchi et al., 1998; Nilius, 1990; Nilius et al., 1993; Nilius et al., 1997). However, the gating mechanism of NSC is still unclear and its molecular identity is still unresolved. We describe here the biophysical and gating properties of an NSC-activated by vasoactive agonists in Ea.hy926 (EA) cells, an endothelial cell line derived from human umbilical vein, which may play a functional role as a pathway for Ca^{2+} entry during agonist stimulation.

Materials and Methods

Cell Culture

A permanent human cell line, Ea.hy926 (EA) cells, established by hybridization of human umbilical vein EC (Edgell, McDonald & Gra-

Correspondence to: B. Nilius

ham, 1983) was grown in DMEM containing 20% fetal calf serum plus 10% HAT 50X supplement (Life Technologies). Cell culture was maintained at 37°C in a fully humidified atmosphere of 10% CO_2 in air. The cells were then detached by exposure to 0.05% trypsin in a Ca^{2+} and Mg^{2+}-free solution, re-seeded on gelatine-coated cover slips, and kept in culture for 2–4 days before use. Measurements were performed on nonconfluent cells.

Electrophysiology

Details of the electrophysiological methods and Ca^{2+} measurement have been described elsewhere (Nilius et al., 1994). The patch-clamp technique was used in the whole cell, cell-attached, inside-out, outside-out configurations. Whole cell membrane currents were measured using ruptured patches. Currents were monitored with an EPC-9 (List Electronic, Germany).

Holding potential of whole-cell experiments was 0 mV. In some experiments, we applied a ramp voltage pulse from −100 to +100 mV with a duration of 200–400 msec. The currents were recorded at a sampling rate of 1 to 4 kHz. The permeability of monovalent cations relative to that of Na^+ was estimated from the shifts in reversal potential by substituting external Na^+ by these cations according to Eq. 1. The Ca^{2+} permeability was estimated from the shift in reversal potential, V_{Ca}–V_{Na}, (Eq. 2) or from the reversal potential, V_{Ca}, in the presence of high external Ca^{2+} (Eq. 3). For more details *see* (Lewis, 1979).

$$\frac{P_X}{P_{Na}} = \frac{[Na]_o}{[X]_o} * exp\left(\frac{F}{RT}(V_X - V_{Na})\right) \quad (1)$$

$$\frac{P_{Ca}}{P_{Na}} = \frac{[Na]_o}{[Ca]_o} * exp\left(\frac{F}{RT}(V_{Ca} - V_{Na})\right) * \left(1 + exp\left(\frac{F * V_{Ca}}{RT}\right)\right) \quad (2)$$

$$\frac{P_{Ca}}{P_{Na}} = \frac{[Na]_i + P_{Cs}/P_{Na} * [Cs]_i}{4[Ca]_o} * exp\left(\frac{F * V_{Ca}}{RT}\right) * \left(1 + exp\left(\frac{F * V_{Ca}}{RT}\right)\right) \quad (3)$$

V_{Na}, V_S and V_{Ca} are reversal potentials measured under the respective conditions described below.

Solutions

The standard external solution (Krebs solution) contained (in mM) 150 NaCl, 10 HEPES, 10 glucose and 1.5 $CaCl_2$. In the solution with high Ca^{2+}, 20 $CaCl_2$ was added and NaCl was reduced by an equimolar amount. For studying permeability of cations, NaCl was replaced by equimolar amounts of CsCl or NMDG/HCl. The internal high Cs^+ pipette solution contained (in mM): 145 Ca-glutamate, 8 NaCl, 2 $MgCl_2$, 10 HEPES, 1 Na_2ATP and buffered with CsOH to 7.2. For buffering free Ca^{2+}, the appropriate amount of Ca^{2+} (calculated by the program CaBuf, G. Droogmans) was added in the presence of 5 mM EGTA or 10 mM BAPTA. In the experiments where we recorded the changes in $[Ca^{2+}]_i$, the pipette solution contained 0.1 mM EGTA. The pH of the extracellular solutions was adjusted to 7.4 with either NaOH or CsOH, the internal solution was buffered at 7.2 with CsOH. The osmolality of all solutions was measured with an osmometer (Wescor 5500 osmometer, Schlag Instruments, Gladbach, Germany).

For single-channel recording, the pipette solution contained (in mM): 140 CsCl, 2 $MgCl_2$, 10 HEPES and 10 TEACl. In some experiments, 140 CsCl was replaced by an equimolar amount of Na glutamate. In cell-attached configuration, the cells were bathed with 150 K^+ solution containing (in mM): 145 KCl, 2 $MgCl_2$ and 10 HEPES. In the inside-out configuration, free Ca^{2+} was buffered at 100 nM. The pH of high K^+ solution was adjusted to 7.4 with KOH for the cell-attached configuration and to 7.2 for inside-out patches, that of the pipette solutions to 7.4 with either CsOH or NaOH.

The major endogenous currents of EA cells that would mask I_{NSC} were eliminated. The large conductance Ca^{2+} activated K^+ channels (Viana et al., 1998) were abolished by removing K^+ from both sides of the membrane and by including Cs^+ (whole cell recording) or TEA (single-channel recording) in the pipette solution. To eliminate volume-activated Cl currents, we have increased the osmolality of all external solutions to 390 ± 5 mosmol/kg by adding mannitol to (Voets, Droogmans & Nilius, 1996). ATP, bradykinin, histamine and TEA (Sigma, St. Louis, MO) were added to the external solution and inositol 1,4,5-trisphosphate ($Ins(1,4,5)P_3$) to the internal solution. U-73122, U-73343 (Calbiochem, La Jolla, CA) and 2,5-di-*tert*-butylhydroquinone (BHQ, Sigma) were dissolved in DMSO as a stock solution and the final concentration of DMSO was less than 0.05%.

Ca^{2+} Measurement

For $[Ca^{2+}]_i$ measurement, cells were loaded with fura-2/AM (the acetoxymethyl ester form). Fura-2/AM (2 μM) was added to the bath and the cells were incubated for 25 min at 37°C. After loading, cells were washed with Krebs solution. The loaded cells were illuminated at wavelengths of 360 and 390 nm through a rotating filter wheel. The fluorescence was measured at 510 nm and the auto fluorescence was subtracted from the signals. Apparent free Ca^{2+} concentration was calculated from the fluorescence ratio *R:*

$$[Ca^{2+}]_i = K_{eff}\frac{(R - R_0)}{(R_1 - R)}$$

where K_{eff} is the effective binding constant, R_o the fluorescence ratio at zero calcium and R_1 that at high Ca^{2+}.

All experiments were performed at room temperature (20–22°C). Pooled data are given as mean ± SEM.

Results

Biophysical Properties

Kinetics

The vasoactive agonists ATP, bradykinin, and histamine, evoked with a rather long latency (1–5 min) large inward and outward currents in EA cells. Kinetics and voltage-dependence of this current were assessed from voltage steps applied after the current has completely developed. The current was time-independent at each potential and did not inactivate during the voltage steps, as shown for ATP (Fig. 1*A*), histamine (Fig. 1*C*) and bradykinin (Fig. 1*E*). The reversal potentials of these currents were close to 0 mV. The current-voltage relationships showed no rectification (Fig. 1*B*). Replacement of external Na^+ with $NMDG^+$ abolished the inward current but had almost no effect on the outward current (Fig. 1*A*). Similar data were obtained in cells stimulated with histamine (Fig. 1*C* and *D*) and bradykinin (Fig. 1*E* and *F*). Therefore, these results suggest that these agonists activate a

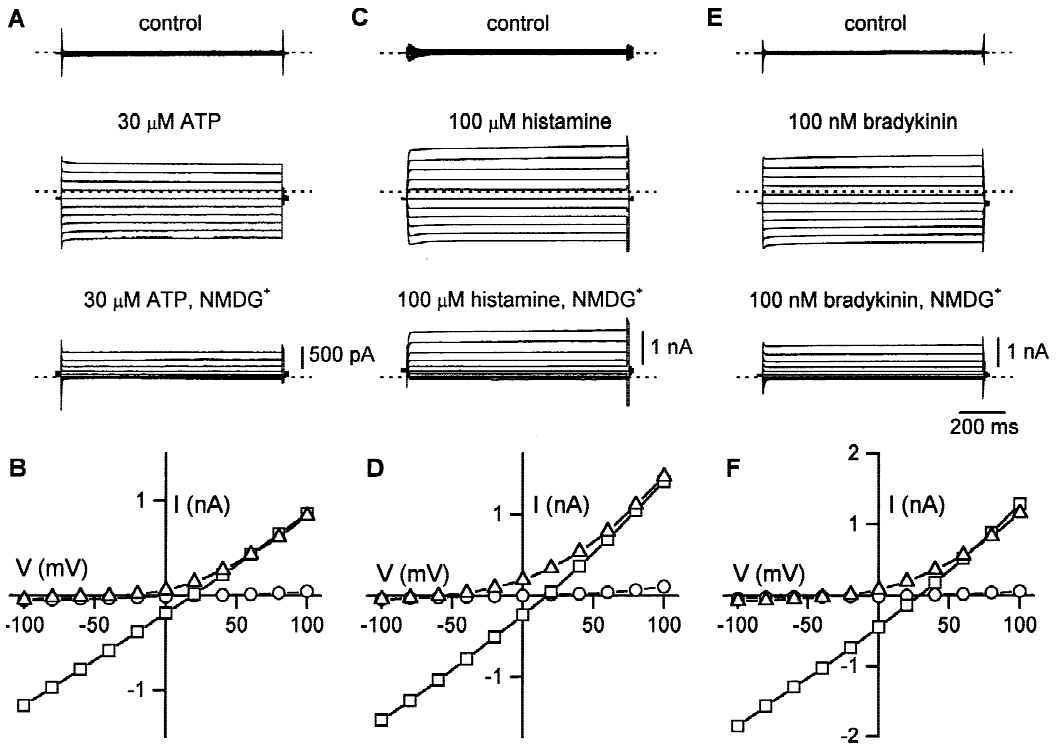

Fig. 1. Agonist-activated cation currents, I_{NSC}. (*A, C, E*) Current traces obtained before (top traces) and after application of agonists (middle and bottom traces). The current was induced by voltage steps of 1 sec to potentials ranging from −100 to 100 mV with an increment of 20 mV. Dotted lines indicate zero current level. The internal solution was Cs^+ glutamate solution. The top and middle traces were obtained in a 150 mM Na^+ bath solution, in the bottom traces external Na^+ was replaced with $NMDG^+$. The current in the middle and bottom traces was recorded in the presence of 30 μM ATP (*A*), 100 μM histamine (*C*) or 100 nM bradykinin (*E*). (*B, D, F*) *I-V* relationships obtained from the currents in *A, C* and *E*, respectively. The current amplitude was measured at the end of the voltage step. Each symbol represents the current amplitude recorded before (circles) and after application of agonists in 150 mM Na^+ solution (squares) or in 150 mM $NMDG^+$ solution (triangles).

time and voltage independent nonselective cation current, I_{NSC}, in EA cells.

Cation Selectivity and Modulation by Di- and Trivalent Cations

The permeability for the cations Cs^+ and $NMDG^+$ relative to that of Na^+ were assessed from the shifts in reversal potential of I_{NSC} by substitution of external Na^+ with these cations. These reversal potentials were obtained from *I-V* relationships reconstructed from voltage ramp pulses. Substitution of external Na^+ with Cs^+ reduced the amplitude of the inward current and shifted the reversal potential of the current from 21.1 ± 2.5 mV in 150 mM Na^+ solution to 12.6 ± 2.3 mV in 150 mM Cs^+ solution ($n = 14$). The permeability ratio P_{Cs}/P_{Na} calculated from this shift using Eq. 1 was 0.72 ± 0.03 ($n = 14$). It was not possible to use a similar procedure to calculate the relative permeability for K^+ because the NSC-current is masked by a large conductance Ca^{2+} activated K^+ current if extracellular Na^+ is replaced by K^+ (Viana et al., 1998).

ATP still activated a current if extracellular NaCl was substituted by an equimolar amount of $CaCl_2$. Its inward component was however much smaller and its reversal potential was shifted to more negative values. The permeability ratio P_{Ca}/P_{Na} calculated from the shift in reversal potential (Eq. 2) was 0.07 ± 0.01 ($n = 5$). This ratio, assessed from the reversal potential measured in high external Ca^{2+} solution using Eq. 3 was 0.11 ± 0.03 ($n = 7$).

Increasing extracellular Ca^{2+} from 1.5 to 20 mM reduced I_{NSC} to 88 ± 3% at −50 mV, a finding that also has been described for other Ca^{2+} permeable NSCs. External Mg^{2+} (1 mM) did not affect the current in the presence of Ca^{2+}, but it induced in Ca^{2+} free solution a weak reduction of the current to 93 ± 2% of its control value at −50 mV ($n = 5$). The reduction of the current by increasing external Ca^{2+} was however always accompanied by an elevation of $[Ca^{2+}]_i$ which strongly suggest that NSC provides a Ca^{2+} entry pathway.

In the presence of 20 mM Ca^{2+}, I_{NSC} was also neither inhibited by 1 mM La^{3+} (101 ± 1% of the control, $n = 5$) nor by 1 mM Gd^{3+} (100 ± 1%, $n = 4$). However, La^{3+}

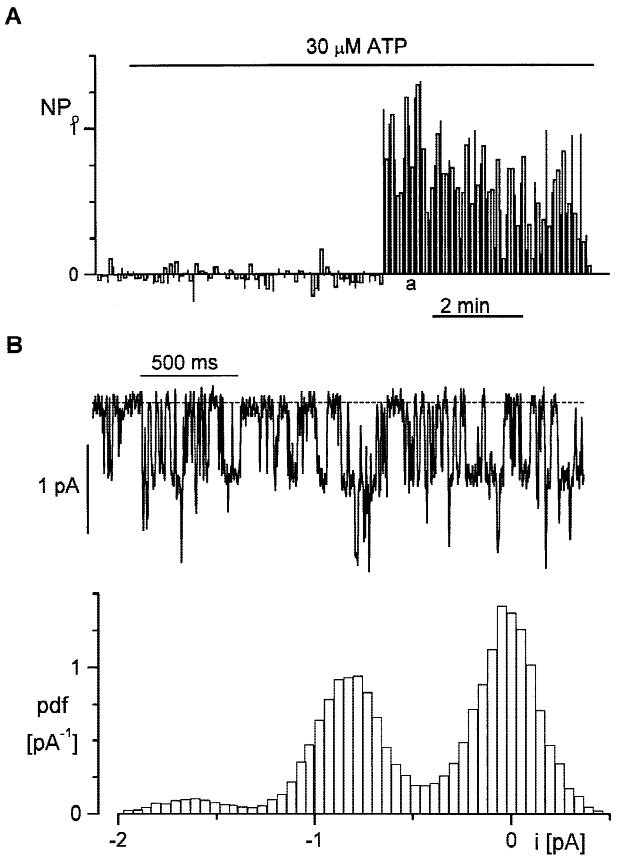

Fig. 2. Single channel current activated by ATP. (*A*) Time course of the channel activity evoked by ATP in cell-attached configuration at a holding potential of −40 mV. The pipette contained Na^+ glutamate solution and the bath was perfused with a KCl solution. ATP was applied to the bath during the period indicated by the horizontal bar. Current was recorded at 2 KHz and filtered at 500 Hz. Channel activity in the ordinate was assessed from NP_o, i.e., the average current per 512-point sweep divided by the single channel current amplitude. Time between traces is 20 sec. (*B*) Current traces recorded at the period labeled a in panel *A* and its corresponding amplitude histogram. The dashed line indicates the zero current level. The single-channel current and open probability calculated from the histogram were 0.81 pA and 0.49, respectively.

and Gd^{3+} dose-dependently blocked the current if external Ca^{2+} was removed. The current amplitude was reduced in Ca^{2+} free solution to 70 ± 13 (n = 3) and 42 ± 9% (n = 6) by 100 μM and 1 mM La^{3+}, respectively. Similarly, 100 μM and 1 mM Gd^{3+} reduced the current at −50 mV to 45 ± 6 (n = 6) and 12 ± 3% (n = 7) of the control values. Therefore, divalent cations have only minor effects on NSC, and rather high concentrations of Gd^{3+} and La^{3+} effectively inhibit the current but only in the absence of external Ca^{2+}.

Single-Channel Properties

In the cell-attached patch configuration, bath application of ATP induced single-channel activity with a long delay in the same range as that observed for the whole cell current (Fig. 2). The single-channel conductance measured in cell-attached mode with 150 mM NaCl in the pipette was 26 ± 2.1 pS (n = 4, Fig. 3, *A* and *B*). The reversal potential of the single-channel current was −9.1 ± 3.1 mV (n = 4), as expected for a nonselective cation channel. Substituting CsCl in the pipette (Fig. 4*A*) by Na glutamate (Fig. 4*B*) did neither affect the reversal potential (−5.1 ± 1.2 mV (n = 4) vs. −6.0 ± 2.0 mV (n = 6)) nor the single channel conductance (23.8 ± 2.4 pS (n = 4) compared to 27.1 ± 2.7 pS (n = 6)). This lack of glutamate effect suggests that the agonist-activated channel is not an anion channel, but rather a nonselective cation channel. The *I-V* relationship of the channel was also examined in inside-out and outside-out configurations under conditions that pipette and bath contained Na^+-glutamate and KCl solution, respectively. In inside-out patches, the measurement was performed before channel run down (Fig. 4*C*). Neither the reversal potential nor the single channel conductance were significantly different from the values in cell-attached configuration (20.0 ± 1.4 pS and −15.9 ± 5.3 mV in 4 inside-out patches and 29.1 ± 2.6 pS and −9.5 ± 5.4 mV in 3 outside-out patches, Fig. 4*D*). If Na^+ was replaced by $NMDG^+$ at the inner surface of the inside-out patch membrane, the outward current at 50 mV was immediately abolished whereas re-substitution of $NMDG^+$ by Na^+ restored the outward current (Fig. 5). These results indicate that ATP activates in EA cells a nonselective cation channel with a conductance of approximately 25 pS.

Gating Mechanism

In cells where $[Ca^{2+}]_i$ was not buffered, the slowly activating I_{NSC} was observed in 19 out of 29 cells stimulated with 30 μM ATP. The current started to develop with a delay of 105 ± 16 sec and reached its peak amplitude 503 ± 67 sec later. The Na^+ inward current density activated by 30 μM ATP at −50 mV was −19.1 ± 2.4 pA/pF (n = 19) and −5.3 ± 0.8 pA/pF (n = 10) by 1 μM ATP. Since ATP exerts its action via P_{2Y2} receptors linked to phospholipase C (PLC) (Viana et al., 1998), it was not surprising that the PLC inhibitor, U-73122 blocked the ATP-induced I_{NSC} (87 ± 7% inhibition at 2 μM, n = 4, 23 ± 4% at 0.3 μM). The inactive analogue, U-73343 (2 μM) was ineffective (*data not shown*, n = 4 cells). We have also tested the effects of U-73122 on the Ca^{2+} plateau in nonvoltage-clamped cells during stimulation with 10 μM ATP (*see also* Viana et al., 1998). When U-73122 (2 μM) was administrated one to two minutes after stimulation with ATP to activate NSC, the plateau rise in $[Ca^{2+}]_i$ was inhibited by 92 ± 5% (n = 4), whereas at a concentration of 0.3 μM the plateau was reduced by 24% (n = 1). U-73343 was ineffective. These data strongly suggest that NSC plays a role

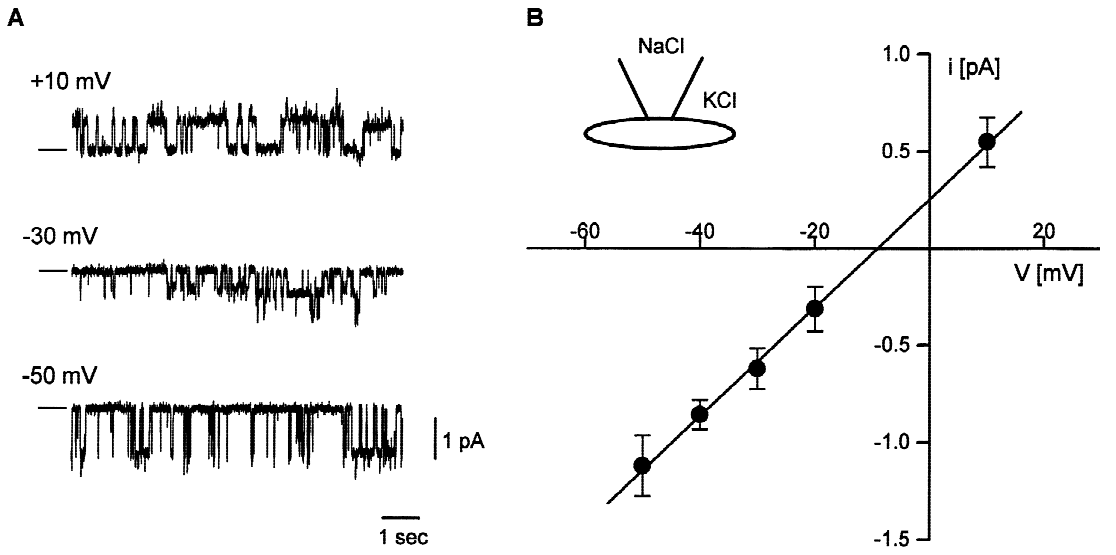

Fig. 3. Single-channel properties of ATP-activated NSC. (*A*) Single-channel current activated by ATP in cell-attached configuration. Current traces were recorded at various potentials 6 min after application of 20 μM ATP (sampling rate 2 KHz, filter at 500 Hz). Dashes indicate the zero current level. (*B*) *I-V* relation of ATP-activated channels. Pipette solution is normal Krebs. The average of the current amplitude obtained from 4 cells was plotted against the holding potential. The continuous line represents the linear fit for the data with a single channel conductance of 26 pS for and a reversal potential −9.

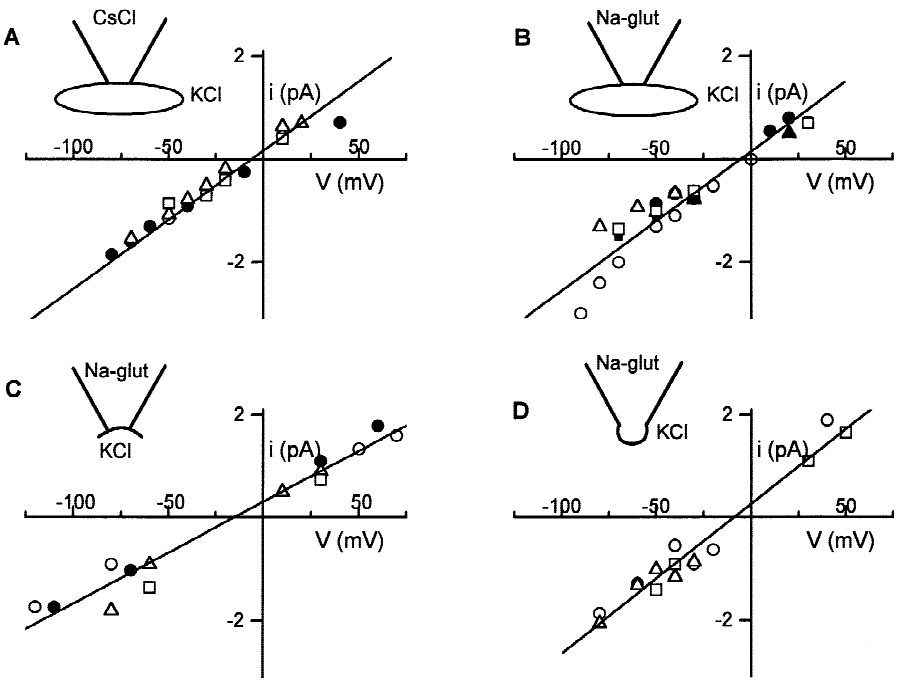

Fig. 4. Permeation properties of ATP-activated NSC. (*A* and *B*) *I-V* relationships obtained in different patches in cell-attached configuration with pipette solutions that contained either CsCl (*A*) or Na glutamate (*B*). The cells were perfused with KCl solution. (*C* and *D*) *I-V* curves in inside-out (*C*) and outside-out configuration (*D*) with pipette solutions that contained Na^+ glutamate solution, and a KCl bath solution. The current amplitude was estimated from amplitude histograms. Different symbols represent different cells. Continuous lines indicate the linear regression through to the data points.

in maintaining the Ca^{2+} plateau during agonist application.

In cells internally perfused with 10 μM $Ins(1,4,5)P_3$ (added the pipette solution) I_{NSC} was activated in 6 out of 8 cells (−22.2 ± 4.7 pA/pF) with a delay of 367 ± 53 sec and reaching a steady-state level 433 ± 71 sec ($n = 6$) later. Also the Ca^{2+}-ATPase inhibitor BHQ (20 μM) activated I_{NSC} in 6 out of 9 cells. The mean Na^+ inward

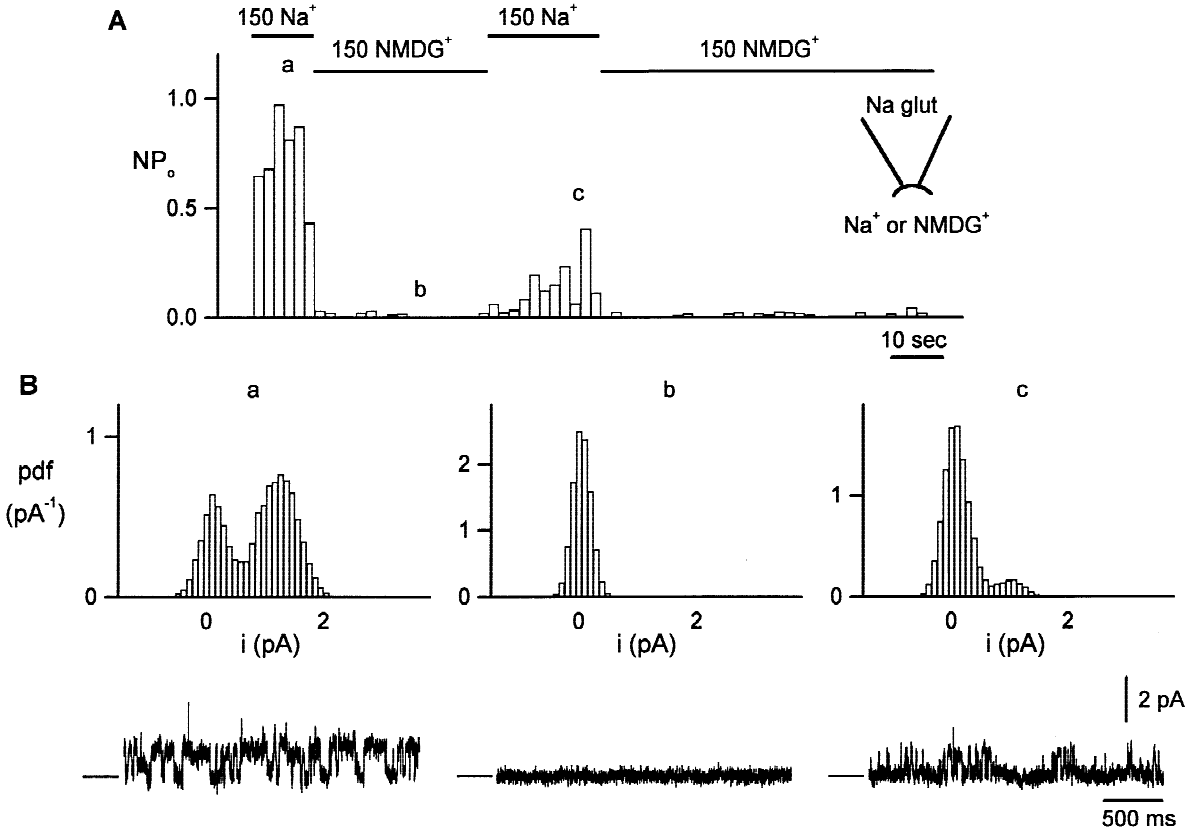

Fig. 5. Permeation of monovalent cations in ATP-activated NSC. (*A*) Time course of the single-channel current in inside-out patches exposed to 150 mM Na^+ solution or 150 mM $NMDG^+$ solution. The current was activated by 10 μM ATP in cell-attached configuration before excising the membrane. The holding potential was 30 mV. Pipette contained Na glutamate solution and the bath was perfused by KCl solution containing 100 nM Ca^{2+}. Single-channel activity was assessed from the average current in 512-point sweeps by 20 sec. (*B*) Amplitude histograms and current traces obtained at different times labeled *a-c* in *A*. Histograms are calculated from 5-sec sweeps recorded at 4 KHz and filtered at 500 Hz. Dashes indicate the zero current level. The single-channel current and NP_o as calculated from histogram from a were 1.1 pA and 0.667, and 0.97 pA and 0.124 from histogram from *c*.

current amplitude activated by BHQ was −24.1 ± 5.8 pA/pF (n = 6). The average delay and time to peak amplitude were 397 ± 59 sec and 367 ± 63 sec (n = 6), respectively. It is however not clear whether activation by these procedures is linked to store depletion rather than to the concomitant changes in $[Ca^{2+}]_i$. If we monitored the changes in $[Ca^{2+}]_i$ together with the membrane current (Fig. 6) and removed extracellular Ca^{2+} after full activation of I_{NSC}, its amplitude and $[Ca^{2+}]_i$ declined, whereas re-addition of Ca^{2+} restored both current and $[Ca^{2+}]_i$ (Fig. 6, *A–C*). Also if $[Ca^{2+}]_i$ was buffered by 10 mM BAPTA at extreme low values, neither of the above procedures did activate I_{NSC} (ATP in 5 cells, $Ins(1,4,5)P_3$ in 15 cells and BHQ in 5 cells). Also no current was activated in cells internally perfused with $Ins(1,4,5)P_3$ with a pipette solution that contained 1 mM EGTA (n = 6).

On the other hand, if the pipette solution was buffered at 1 μM $[Ca^{2+}]_i$, 1 μM ATP elicited a current with an amplitude of −19.8 ± 3.3 pA/pF (n = 14), which is significantly larger than that induced by the same ATP-concentration in non Ca^{2+}-buffered cells (*see above*, −5.3 ± 0.8 pA/pF, n = 10). The delay (127 ± 26 sec) and the time to peak (613 ± 76 sec) were similar to that in non-buffered cells. BHQ also activated I_{NSC} in 6 out of 8 cells (−28.2 ± 7.7 pA/pF, n = 6) with a latency of 225 ± 38 sec (Fig. 7).

Surprisingly, increasing $[Ca^{2+}]_i$ to 1 μM led to a spontaneous activation of the current in 8 out of 17 cells. However, the time course of the spontaneously activated current seems to be slower (delay 207 ± 47 sec time to peak 869 ± 214 sec, n = 8) and also its amplitude is smaller (−11.1 ± 2.4 pA/pF, n = 8). In the other cells where high $[Ca^{2+}]_i$ failed to activate the current, ATP and BHQ could still evoke it. The PLC inhibitor U-73122 but not its inactive analogue U-73343 blocked the current spontaneously activated by the increase in $[Ca^{2+}]_i$ (n = 5 cells).

A synopsis of the various activation protocols for NSC is depicted in Fig. 8.

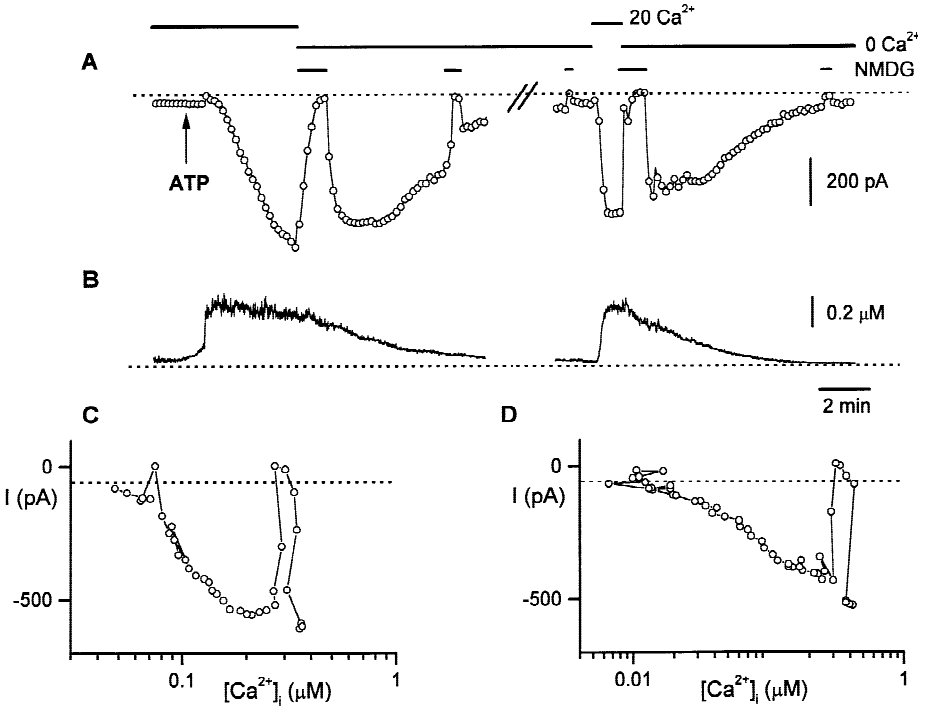

Fig. 6. Role of $[Ca^{2+}]_i$ in I_{NSC}. (*A* and *B*) $[Ca^{2+}]_i$ and membrane current measured simultaneously in a non Ca^{2+}-buffered cell. The upper traces (*A*) indicate the time course of the membrane current at −50 mV, lower traces the change in $[Ca^{2+}]_i$ measured using fura-2 fluorescence (*B*). ATP (30 μM) was added to the external solution at the time indicated by the arrow. The extracellular Ca^{2+} concentration is indicated above the traces and strongly affects the current amplitude. (*C* and *D*) Changes in the ATP-activated current related to the changes in $[Ca^{2+}]_i$ at −50 mV. Internal Na^+ glutamate solution contained 0.1 mM EGTA. External solution was 150 mM Na^+ or 150 mM $NMDG^+$ solution.

Discussion

We have described properties of a NSC that can be activated by vasoactive agonists in EA cells, endothelial cells derived from human umbilical vein. NSCs have already been observed in primary cultured endothelial cells (HUVEC) but have not been further characterized (Nilius, 1990; Gericke, Droogmans & Nilius, 1993; Nilius et al., 1993), although such a characterization might be important because of a possible link with *trp* encoded Ca^{2+} entry channels (Kamouchi et al., 1998).

The main biophysical characteristics of NSC in EA cells are its voltage-independent activation, its permeability sequence $P_{Na} > P_{Cs} >> P_{Ca}$, the weak blocking effect of divalent and trivalent cations and a single-channel conductance of about 25 pS. A similar voltage independence has been reported for other EC (for a review *see* Nilius et al., 1997), but is in contrast with the observation that histamine-operated NSC in rat intrapulmonary arterial EC are activated by depolarization (Yamamoto et al., 1992) and that the NSCs activated by hypotonic shock in bovine aortic EC can also be activated by hyperpolarisation (Ling & O'Neill, 1992).

The higher permeability for Na^+ than for Cs^+ in NSC of EA cells is at variance with the findings for the background NSC in bovine pulmonary arterial EC (Voets et al., 1996), the substance P-activated NSC in coronary arterial EC (Sharma & Davis, 1995) and the background NSC in endocardial cells (Manabe, Takano & Noma, 1995), but the same as for the ATP-activated NSC in endocardial cell (Manabe et al., 1995). The relative permeability for Ca^{2+} over monovalent cations in NSC in EA cells is much smaller than that reported for the histamine-operated NSC in intrapulmonary artery (P_{Ca}/P_{Na} = 15.7, (Yamamoto et al., 1992)), the substance P-activated NSC in coronary arterial EC (P_{Ca}/P_{Cs} = 8, (Sharma & Davis, 1995)) and the stretch-activated NSC in porcine aortic EC (P_{Ca}/P_{Na} = 6, (Lansman, Hallam & Rink, 1987)). It is however similar to that of the Ca^{2+}-dependent NSC in porcine aortic EC (P_{Ca}/P_{Na} = 0.7, (Baron et al., 1996)), the histamine-activated NSC in human umbilical vein EC (P_{Ca}/P_K = 0.2, (Nilius, 1990) and the background NSC in endocardial cell (P_{Ca}/P_K = 0.57, (Manabe et al., 1995)).

Also the blocking effects of divalent and trivalent cations on NSC in endothelial cells seem to be very tissue specific. It has been reported that both intra- and extracellular Mg^{2+} cause a voltage-dependent block of NSC activated by histamine in rat intrapulmonary arterial EC (Manabe et al., 1995). Our observations of a

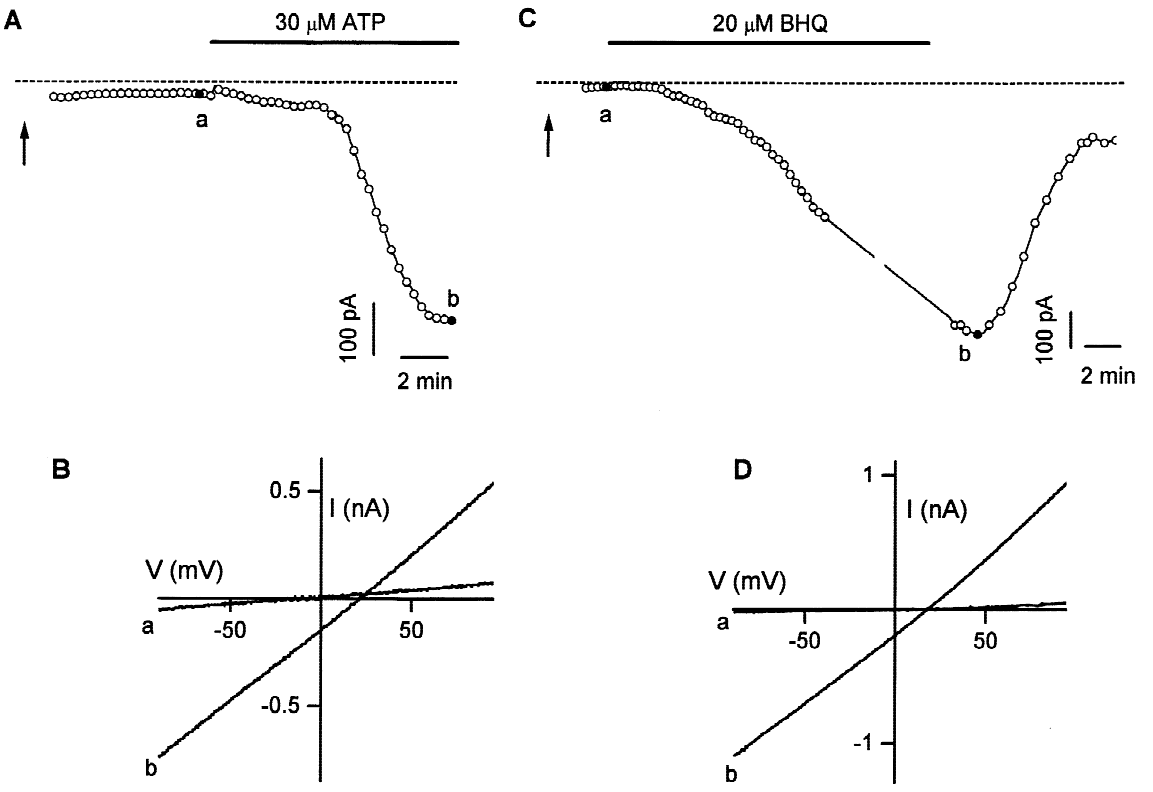

Fig. 7. Effects of ATP and BHQ on I_{NSC}. (*A* and *C*) time course of the current activated at −50 mV by 30 μM ATP (*A*) or 20 μM BHQ (*B*). The internal Ca^{2+} concentration, $[Ca^{2+}]_i$, was clamped at 1 μM and the cells were exposed to 150 mM Na^+ solution containing 20 mM Ca^{2+}. The whole-cell configuration was made at the time indicated by arrows. (*B* and *D*) corresponding *I-V* curves recorded at the times labeled *a* and *b* in *A* and *C*. ATP and BHQ were applied to the bath during the period indicated by the horizontal bars above the traces. Internal and external solutions were Na^+ glutamate and 150 mM Na^+, respectively.

rather weak blocking effect of divalent and trivalent cations in the presence of extracellular Ca^{2+} might be due to competition of these cations with Ca^{2+} for a site that binds Ca^{2+} with much higher affinity. The block by Gd^{3+} and La^{3+} in the absence of extracellular Ca^{2+} is similar to the effect that Gd^{3+} exerts on the background NSC in endocardial cell (Manabe et al., 1995), on the Ca^{2+} and ATP sensitive NSC in rat cerebral capillary arterial EC (Popp & Gögelein, 1992) and on the NSC activated by hypotonic shock in bovine aortic EC (Ling & O'Neill, 1992), and to the block by La^{3+} of NSC that has been described in bovine pulmonary arterial EC (Inazu, Zhang & Daniel, 1995).

The single channel conductance of NSC in EA cells for monovalent cations under physiological conditions is in the range reported for other NSC in EC, i.e., between 20 and 50 pS (Nilius et al., 1997).

Gating Mechanisms

Various gating mechanisms of NSC in endothelium have been discussed, such as an increase in $[Ca^{2+}]_i$ (Bregestovski et al., 1988; Nilius, 1990; Baron et al., 1996), mechanical forces (Lansman et al., 1987; Popp & Gogelein, 1992), depletion of intracellular Ca^{2+} stores (Zhang et al., 1994; Pasyk, Inazu & Daniel, 1995; Sharma & Davis, 1995; Davis & Sharma, 1997), oxidant stress (Koliwad, Elliott & Kunze, 1996*a*,*b*) and receptor activation (Nilius et al., 1997).

The present results clearly indicate that $[Ca^{2+}]_i$ in the physiological range plays a major role in NSC activation, although the long delay between the increase in $[Ca^{2+}]_i$ and current activation after agonist application points to an indirect target for Ca^{2+} which is downstream from the channel. However, intracellular Ca^{2+} is not the only gating signal, since the spontaneous activation observed in 8 out of 17 cells buffered at 1 μM $[Ca^{2+}]_i$ is abolished in the presence of PLC inhibitors, and that ATP and BHQ can activate the current in cells where high internal Ca^{2+} failed to induce it. A possible role of $[Ca^{2+}]_i$ may be a sensitisation of the binding of $Ins(1,4,5)P_3$ to its receptor (Michikawa et al., 1996), thereby potentiating the effect of endogenous $Ins(1,4,5)P_3$. However, Ca^{2+} may also play a role in the membrane attachment and hydrolysis of phosphoinositides by PLC (Essen et al., 1996).

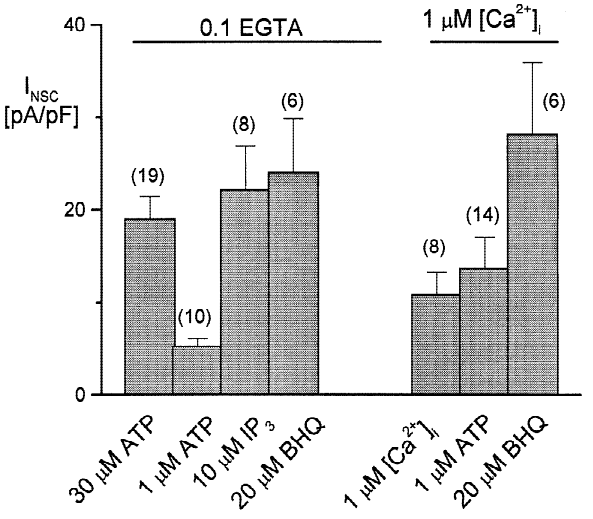

Fig. 8. Synopsis of the protocols used to activate I_{NSC}. Bars represent the inward current density at −50 mV as observed for the various procedures and for two different experimental conditions, i.e., cells without $[Ca^{2+}]_i$ buffering (0.1 mM EGTA in the patch pipette) or cells with $[Ca^{2+}]_i$ buffered at 1 μM. Note that 1 μM $[Ca^{2+}]_i$ by itself activated the current in 8 of 17 cells. The number of cells is indicated for each protocol above the corresponding column.

It has been reported that store depletion by Ca^{2+}-ATPase inhibitors induces I_{NSC} in human umbilical vein EC (Gericke et al., 1993; Zhang et al., 1994), bovine pulmonary arterial EC (Pasyk et al., 1995) and pig coronary arterial EC (Sharma & Davis, 1995; Davis & Sharma, 1997). These observations and our present results are consistent with a store depletion-dependent activation of NSC. However, our observation that all procedures that induces store depletion, such as stimulation with ATP, internal perfusion with Ins(1,4,5)P_3 and application of BHQ failed to activate NSC if intracellular Ca^{2+} was buffered at extreme low values with 10 mM BAPTA is not consistent with an activation mechanism that is controlled by the filling degree of internal Ca^{2+} stores only. Intracellular Ca^{2+} is at least an important cofactor, such as described for CRAC channels in T lymphocytes (Zweifach & Lewis, 1996), which exerts an important positive feedback on the channel activity, such as reported for depletion-activated channels in *Xenopus* oocytes.

Physiological Role of NSC in Endothelium

We have shown that NSC is an agonist-activated Ca^{2+}-permeable channel and that inhibition of these channels decreases the agonist-induced Ca^{2+} plateau (*see also* Viana et al., 1998). These properties strongly suggest that activation of NSCs increases $[Ca^{2+}]_i$ and may therefore play a role as a Ca^{2+} influx pathway which is responsible for the maintained (plateau) elevation of $[Ca^{2+}]_i$ during agonist stimulation. Because the sustained plateau is a necessary condition for essential endothelial functions, such as secretion of prostacyclin (PGI_2), nitric oxide (NO), tissue plasminogen activator (tPA), platelet activating factor (PAF), von Willebrand factor (vWF), tissue factor pathway inhibitor (TFPI), etc. (Inagami et al., 1995; Iouzalen et al., 1996; Lantoine et al., 1998) (Jacob et al., 1988; Jacob, 1990; Carter & Ogden, 1992; Nilius et al., 1997), NSC may be of significant functional importance. Importantly, $[Ca^{2+}]_i$ does not inactivate but activate NSC, and may have a positive feedback effect on the transmembrane Ca^{2+} influx via NSC. Such a pathway could play an important role to sustain a long-lasting Ca^{2+} plateau. CRAC would be a less suitable candidate for such a function because it is inactivated by an increase in $[Ca^{2+}]_i$.

In conclusion, we have identified and characterized a nonselective cation channel, NSC, in endothelium which may function as a Ca^{2+} influx pathway. NSC is Ca^{2+} sensitive, and its gating might require the convergent action of several mechanisms, including Ins(1,4,5)P_3 binding and possibly store depletion.

We thank Dr. Edgell for the gift of EA cells. M.K. was supported by a fellowship from the Onderzoeksfonds KU Leuven, the F.W.O., Belgium and European Commission and A.M. from INTAS and the F.W.O., Belgium. We thank Drs. C. Fasolato and F. Viana for their helpful suggestions and J. Prenen for his technical assistance. We are grateful to A. Florizone and M. Crabbé for performing the cell cultures. This work was supported by the Federal Belgian State (Interuniversity Poles of Attraction Programme, Prime Ministers Office IUAP Nr.3P4/23), the Flemish Government (F.W.O. G.0237.95, C.O.F./96/22-A0659), and by the European Commission (BMH4-CT96-0602) and INTAS (94-0241).

References

Baron, A., Frieden, M., Chabaud, F., Bény, J.-L. 1996. Ca^{2+}-dependent nonselective cation and potassium channels activated by bradykinin in pig coronary artery endothelial cells. *J. Physiol.* **493:**691–706

Berridge, M.J. 1995. Capacitive calcium entry. *Biochem. J.* **312:**1–11

Bregestovski, P., Bakhramov, A., Danilov, S., Moldobaeva, A., Takeda, K. 1988. Histamine-induced inward currents in cultured endothelial cells from human umbilical vein. *Brit. J. Pharmacol.* **95:**429–436

Carter, T.D., Ogden, D. 1992. Kinetics of intracellular calcium release by inositol 1,4, 5-trisphophate and extracellular ATP in porcine cultured aortic endothelial cells. *Proc. of the Royal Soc London. Series B: Biological Science* **250:**235–241

Clapham, D.E. 1995. Calcium signaling. *Cell* **80:**259–268

Davis, M.J., Sharma, N.R. 1997. Calcium-release-activated calcium influx in endothelium. *J. Vasc. Res.* **34:**186–195

Edgell, C.-J.S., McDonald, C.C., Graham, J.B. 1983. Permanent cell line expressing human factor VIII-related antigen established by hybridization. *Proc. Nat. Acad. Sci. USA* **80:**3734–3737

Essen, L.-O., Perisic, O., Cheung, R., Katan, M., Williams, R.L. 1996. Crystal structure of a mammalian phosphoinositide-specific phospholipaseCδ. *Nature* **380:**595–602

Fasolato, C., Nilius, B. 1998. Store depletion triggers the calcium release-activated calcium current (I_{CRAC}) in macrovascular endothe-

lial cells: a comparison with Jurkat and embryonic kidney cell lines. *Pfluegers Arch.* **436:**69–74

Gericke, M., Droogmans, G., Nilius, B. 1993. Thapsigargin discharges intracellular calcium stores and induces transmembrane currents in human endothelial cells. *Pfluegers Arch.* **422:**552–557

Hoth, M., Penner, R. 1992. Depletion of intracellular calcium stores activates a calcium current in mast cells. *Nature* **355:**353–356.

Hoth, M., Penner, R. 1993. Calcium release-activated calcium current in rat mast cells. *J. Physiol.* **465:**359–386

Inagami, T., Naruse, M., Hoover, R. 1995. Endothelium: As an endocrine organ. *Ann. Rev. Physiol.* **57:**171–189

Inazu, M., Zhang, H., Daniel, E.E. 1995. Different mechanisms can activate Ca^{2+} entrance via cation currents in endothelial cells. *Life Sciences* **56:**11–7

Iouzalen, L., Lantoine, F., Pernollet, M.G., Millanvoye-Van-Brussel, E., Devynck, M.A., David-Dufilho, M. 1996. SK&F 96365 inhibits intracellular Ca^{2+} pumps and raises cytosolic Ca^{2+} concentration without production of nitric oxide and von Willebrand factor. *Cell Calcium* **20:**501–508

Jacob, R. 1990. Agonist-stimulated divalent cation entry into single cultured human umbilical vein endothelial cells. *J. Physiol.* **421:**55–77

Jacob, R., Merritt, J.E., Hallam, T.J., Rink, T.J. 1988. Repetitive spikes in cytoplasmic calcium evoked by histamine in human endothelial cells. *Nature* **335:**40–5

Kamouchi, M., Philipp, S., Flockerzi, V., Raeymaekers, L., Eggermont, J., Droogmans, G., Nilius, B., Wissenbach, U., Mamin, A. 1999. Properties of heterologously expressed hTRP3 channels in bovine pulmonary artery endothelial cells. *J. Physiol.* (*in press*)

Koliwad, S.K., Elliott, S.J., Kunze, D.L. 1996*a*. Oxidized glutathione mediates cation channel activation in calf vascular endothelial cells during oxidant stress. *J. Physiol.* **495:**37–49

Koliwad, S.K., Kunze, D.L., Elliott, S.J. 1996*b*. Oxidant stress activates a nonselective cation channel responsible for membrane depolarization in calf vascular endothelial cells. *J. Physiol.* **491:**1–12

Lansman, J.B., Hallam, T.J., Rink, T.J. 1987. Single stretch-activated ion channels in vascular endothelial cells as mechanotransducers? *Nature* **325:**811–813

Lantoine, F., Iouzalen, L., Devynck, M.A., Millanvoye-Van-Brussel, E., David-Dufilho, M. 1998. Nitric oxide production in human endothelial cells stimulated by histamine requires Ca^{2+} influx. *Biochem. J.* **330:**695–699

Lewis, C.A. 1979. Ion-concentration dependence of the reversal potential and the single channel conductance of ion channels at the frog neuromuscular junction. *J. Physiol.* **286:**417–445

Ling, B.N., O'Neill, W.C. 1992. Ca^{2+}-dependent and Ca^{2+}-permeable ion channels in aortic endothelial cells. *Am. J. Physiol.* **263:**H1827–H1838

Manabe, K., Takano, M., Noma, A. 1995. Nonselective cation current of guinea-pig endocardial endothelial cells. *J. Physiol.* **487:**407–419

Michikawa, T., Miyawaki, A., Furuichi, T., Mikoshiba, K. 1996. Inositol 1,4,5-trisphosphate receptors and calcium signaling. *Critical Reviews in Neurobiology* **10:**39–55

Nilius, B. 1990. Permeation properties of a nonselective cation channel in human vascular endothelial cells. *Pfluegers Arch.* **416:**609–611

Nilius, B., Oike, M., Zahradnik, I., Droogmans, G. 1994. Activation of a Cl^- current by hypotonic volume increase in human endothelial cells. *J. Gen. Physiol.* **103:**787–805

Nilius, B., Schwarz, G., Oike, M., Droogmans, G. 1993. Histamine-activated, nonselective cation currents and Ca^{2+} transients in endothelial cells from human umbilical vein. *Pfluegers Arch.* **424:**285–293

Nilius, B., Viana, F., Droogmans, G. 1997. Ion channels in vascular endothelium. *Ann. Rev. Physiol.* **59:**145–170

Nilius, B., Viana, F., Kamouchi, M., Fasolato, C., Eggermont, J., Droogmans, G. 1998. Ca^{2+} signaling in endothelial cells: role of ion channels. *Korean J. Physiol.* **2:**133–145

Oike, M., Gericke, M., Droogmans, G., Nilius, B. 1994. Calcium entry activated by store depletion in human umbilical vein endothelial cells. *Cell Calcium* **16:**367–376

Parekh, A.B., Penner, R. 1997. Store depletion and calcium influx. *Physiol. Rev.* **77:**901–930

Pasyk, E., Inazu, M., Daniel, E.E. 1995. CPA enhances Ca^{2+} entry in cultured bovine pulmonary arterial endothelial cells in an IP_3-independent manner. *Am. J. Physiol.* **268:**H138–H146

Popp, R., Gögelein, H. 1992. A calcium and ATP-sensitive nonselective cation channel in the antiluminal membrane of rat cerebral capillary endothelial cells. *Biochem. Biophys. Acta* **1108:**59–66

Sharma, N.R., Davis, M.J. 1995. Substance P-induced calcium entry in endothelial cells is secondary to depletion of intracellular stores. *Am. J. Physiol.* **268:**H962–H973

Viana, F., De Smedt, H., Droogmans, G., Nilius, B. 1998. Calcium signaling through nucleotide receptor P_{2Y2} in cultured human vascular endothelium. *Cell Calcium* **24:**117–127

Voets, T., Droogmans, G., Nilius, B. 1996. Membrane currents and the resting membrane potential in cultured bovine pulmonary artery endothelial cells. *J. Physiol.* **497:**95–107

Yamamoto, Y., Chen, G., Miwa, K., Suzuki, H. 1992. Permeability and Mg^{2+} blockade of histamine-operated cation channel in endothelial cells of rat intrapulmonary artery. *J. Physiol.* **450:**395–408

Zhang, H., Inazu, M., Weir, B., Buchanan, M., Daniel, E. 1994. Cyclopiazonic acid stimulates Ca^{2+} influx through nonspecific cation channels in endothelial cells. *Eur. J. Pharmacol.* **251:**119–125

Zweifach, A., Lewis, R.S. 1996. Calcium-dependent potentiation of store-operated calcium channels in T lymphocytes. *J. Gen. Physiol.* **107:**597–610